Mathematical modeling of movement and heat transfer of particles of dispersed materials during their processing in a plasma chemical reactor

Nekrasov A.K.[1], Kholpanov L.P.[2], Nekrasova E.I.[3]*

[1]*Moscow State University of Engineering Ecology, Moscow, Russia*
[2]*Institute for Problems of Chemical Physics RAS, Chernogolovka, Russia*
[3]*Elektrostal Polytechnic Institute (MISiS branch), Elektrostal, Russia*

Abstract

In work the mathematical model of hydrodynamics and heat exchange are considered at movement of the nonuniform multiphase heterogeneous environment with disperse spherical particles in conditions of convection in a plasmachemical reactor, and also nonstationary is heat mass transfer at relative movement of a disperse particle and the carrying viscous incompressible environment in view of fusion and evaporation from a surface. The case of small volumetric concentration of particles is considered. The basic attention is given to local dynamic and thermal influence of the carrying environment on particles, and by interaction of particles and their influence on the carrying environment was neglected. For definition of parameters of carrying gas the system of the equations of movement, indissolubility and the energy, written down in approximation of Boussinesq is solved. Definition of parameters of relative movement of disperse particles and the carrying environment is carried out by a method, based on replacement of the vector equation of movement for a particle system of two scalar equations received for the module and a corner of a direction of a vector of relative speed of a particle with variable weight. For definition of a temperature mode and radius of a disperse particle changing at evaporation the non-stationary problem of heat conductivity in a particle of the spherical form is solved in view of fusion and evaporation of a material on a surface.

Keywords: heat exchange; hydrodynamics; dispersible particles; mathematical model

1. Introduction

Recently, with the development of membrane catalysis technologies, increasing interest has been shown in obtaining samples of chromium oxide catalysts in the form of a nanodispersed powder suitable for modifying membranes. A promising technological process for obtaining nanodispersed powders is a plasma-chemical process using high-frequency plasma-chemical installations [1, 2]. The schematic diagram of the plasma-chemical installation from [1] is shown in Figure 1.

The most energy-intensive plasma-chemical processes are the processes of obtaining materials with a new chemical composition. In such technological processes, by intensive supply of thermal energy, the initial dispersed material is evaporated and transferred to the gas phase, and then additional thermal energy is required for the necessary chemical reactions to occur.

The efficiency of processing particulate material in the reactor is determined by various factors. However, as studies and experience in the operation of plasma installations show [3, 4], in most processes of plasma treatment of dispersed materials, the main limiting factor is the heat exchange of a high-temperature gas flow with the particles of the processed material moving in it, as well as the heat exchange of the plasma-forming gas with the walls of the reactor channel.

When designing plasma-chemical apparatuses, in order to select the dimensions of reactors and their operating parameters in order to evaluate possible ways to control processes and product quality, it is necessary to know the general patterns of motion

*Corresponding author
email: nekrasov55@yandex.ru
doi: https://doi.org/10.23877/MS.TS.39.006
Published online: 15 June 2017

and heat transfer of dispersed material and plasma flow in the system plasma flow – dispersed material – reactor channel walls. However, despite the relevance of the problem, studies of the hydrodynamics of the flow of a heterogeneous inhomogeneous medium with dispersed particles and the heat transfer of particles and plasma during their relative motion are still few. The process of obtaining superheated steam during the evaporation of particles of the initial dispersed material is considered one of the main ones. This process is quite complex and the following stages can be distinguished in it: heating of particles to the melting temperature; melting; heating to evaporation temperature; evaporation; cooling of the obtained products [3]

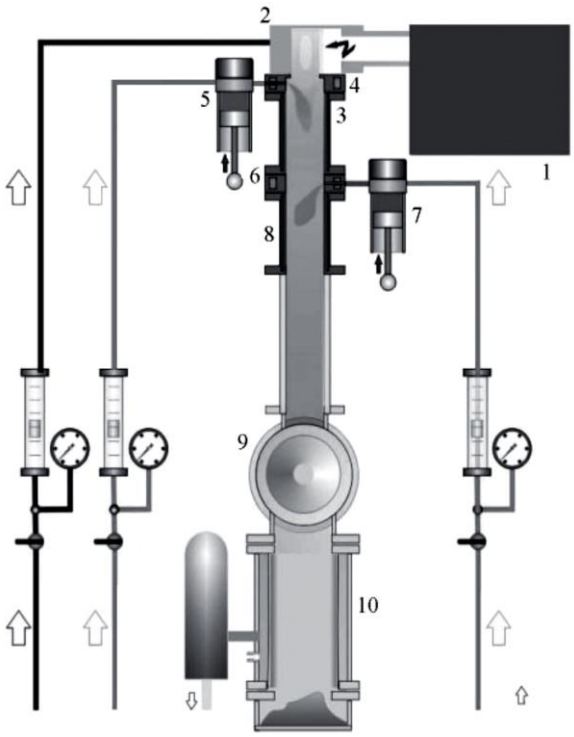

Figure 1 Plasmochemical setup layout [1]: 1 – microwaves' generator; 2 – plasma generator; 3 – high temperature section; 4 – 1st powder injection device; 5 – 1st powder dispenser; 6 – 2nd powder injection device 2; 7 – 2nd powder dispenser; 8 – low temperature section; 9 – heat exchanger; 10 – filter

The duration of the noted stages of processing a dispersed material, which affects the productivity of the processing process and the quality of the final product, is largely determined by the intensity of heat and mass transfer, which depends on the trajectories of the movement of dispersed particles in an inhomogeneous high-temperature carrier medium and their relative speed.

Experimental studies of dynamic and thermal interactions of dispersed particles with a heated gas flow during their relative motion are associated with significant difficulties. This contributes to the active development of mathematical models of hydrodynamics and heat and mass transfer processes that occur during the interfacial interaction of the dispersed and carrier phases, as well as effective numerical methods for their solution [5,6].

2. Materials and methods

This paper considers the hydrodynamics and heat transfer during the motion of an inhomogeneous multiphase heterogeneous medium with dispersed spherical particles under conditions of mixed convection in a reactor, as well as non-stationary heat transfer during the relative motion of a dispersed particle and a carrier viscous incompressible medium, taking into account the

heating of particles to a melting temperature, melting, heating to temperatures of evaporation, evaporation and cooling of the obtained products.

The reactor (Figure 2) is a vertical cylindrical channel with a diameter $D=2R$ and a length L, at the inlet of which gas heated to a temperature T_{10} with a density ρ_1 is supplied from the plasmatron at a speed V_{10} from top to bottom. Simultaneously with the gas, spherical particles of the processed dispersed material with a diameter dp_0 with a density ρ_2 and with initial values of temperature T_{20} and velocity V_{20} are fed into the reactor. The carrier gas flow is axisymmetric, and velocity and temperature profiles at the reactor inlet homogeneous and have average values, respectively, V_{10} and T_{10}. The case of a low volume concentration of particles is considered. The main attention is paid to the local dynamic and thermal effects of the carrier medium on the particles, and the interaction of particles with each other and their influence on the carrier medium were taken to be insignificant.

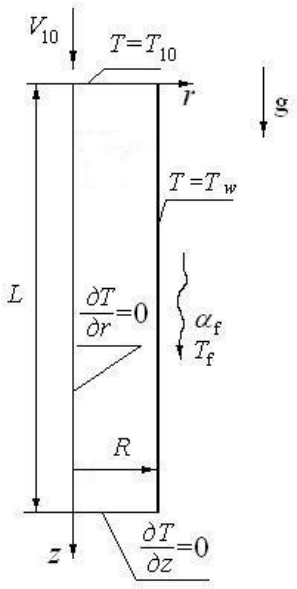

Figure 2 Design scheme of the reactor

At the initial moment of time, the carrier medium in the reactor has a uniform initial temperature T_0. The outer surface of the reactor wall can either be maintained at a temperature constant in time and uniform over the surface T_w, or cooled by a liquid having a temperature constant in time and uniform over the surface T_f at a constant heat transfer coefficient α_f. The thermal resistance of the reactor wall was not taken into account.

For a carrier gas with an inlet velocity of V_{10} and a plasma torch moving in a cylindrical reactor channel with an inner diameter D and a length L, the system of vector equations of motion, continuity, and energy in dimensionless variables relative to the corresponding scales (for space, the inner diameter of the reactor channel, D; for speed – V_{10}, for time – D/V_{10}, for pressure – $\rho_1 \cdot V_{10}^2$, for temperature – ϑ_{w0}) in the Boussinesq approximation has the form [7]:

$$\frac{\partial}{\partial t}\mathrm{V}_1 + (\mathrm{V}_1\nabla)\,\mathrm{V}_1 = -\nabla \mathrm{p} + \frac{1}{\mathrm{Re}}\,\Delta \mathrm{V}_1 + \mathrm{n}\frac{Gr}{\mathrm{Re}^2}\,\theta_1, \quad (1)$$

$$\mathrm{div}\mathbf{V}_1=0, \quad (2)$$

$$\frac{\partial \theta_1}{\partial t} + (\mathbf{V}_1\nabla)\,\theta_1 = \frac{1}{\mathrm{Re}\,\mathrm{Pr}}\,\Delta\theta_1, \quad (3)$$

where $Re = V_{10}D/v$ – Reynolds criterion; $\mathrm{Gr} = gD^3\vartheta_{10}\beta/v^2$ – Grashof criterion; v – kinematic

viscosity coefficient, m²/s; g – acceleration of gravity, m/s²; β – coefficient of thermal expansion, 1/K; **n** – unit vector of gravity direction; $\theta_1 = \vartheta_1/\vartheta_{10}$ – dimensionless temperature; $Pr = \nu/a$ – dimensionless temperature; a – thermal diffusivity, m²/s; $\vartheta_1 = T_1 - T_0$, $\vartheta_{10} = T_{10} - T_0$ – relative temperatures of the carrier medium, respectively, current and at the inlet to the reactor, K.

The boundary conditions for the system (1) – (3) were taken:

$$t = 0: \boldsymbol{V}_1 = 0, \theta_1 = 0, \quad (4)$$

$$r \to 0, 0 \le z \le \frac{L}{D}: \frac{\partial \theta_1}{\partial r} = 0, \quad (5)$$

$$\boldsymbol{V}_1 = 0, r = 0.5, 0 \le z \le \frac{L}{D}: -\frac{\partial \theta_1}{\partial r} = Bi\,(\theta_1 - \theta_f), \quad (6)$$

$$\boldsymbol{V}_1 = 0, z = 0, 0 \le r \le 0.5: \theta_1 = 1, \quad (7)$$

$$\mathbf{V}_1 = 1, z = \frac{L}{D}, 0 \le r \le 0.5: \frac{\partial \theta_1}{\partial z} = 0, \quad (8)$$

$$\frac{\partial}{\partial z}\mathbf{V}_1 = 0$$

here z, r – dimensionless coordinates in space; $Bi = \alpha_f \cdot D/\lambda_1$.

The equation of motion of a particle with varying mass m and diameter d_p has the form [8]

$$m\frac{d}{dt}\mathbf{V}_2 = -0.5C\pi r_p^2 \cdot \rho_1 w^2 \cdot \mathbf{e} + \mathbf{F} + \mathbf{f}, \quad (9)$$

where: t – time, s; C – drag coefficient; $r_p(t) = d_p/2$ – current particle radius, м; $w = |\mathbf{V}_{rel}| = |\mathbf{V}_2 - \mathbf{V}_1|$ – particle relative velocity vector modulus, m/s; $\mathbf{e} = \mathbf{i}\cdot cos\alpha + \mathbf{j}\cdot sin\alpha + \mathbf{k}\cdot 0$ – unit relative velocity direction vector unit relative velocity direction vector; **F** – vector of mass force equal to the sum of gravity and lift of Archimedes; α – rotation angle from coordinate axis r to unit vector **e**; $\mathbf{f} = \frac{dm}{dt}(\mathbf{u} - \mathbf{V}_2)$ – the vector of the impulse force when the particle mass changes; **u** – velocity vector of mass particles during evaporation from the surface.

To determine the parameters of the relative motion of dispersed particles and the carrier medium, the method proposed in [9] is used, according to which, instead of the vector equation (9), a system of two scalar equations is solved for the particle, obtained for the modulus and direction angle of the relative motion velocity vector. The system of dimensionless equations for finding the modulus w and direction angle α of the relative velocity vector for a particle with variable radius and mass has the form:

$$\frac{dw}{dt} = -k_c w^2 - (P_r + E_r - F_r - U\acute{r}) \cdot \cos\alpha - (P_z + E_z - F_z - V\acute{r}) \sin\alpha + w\acute{r}, \quad (10)$$

$$w\frac{d\alpha}{dt} = (P_r + E_r - F_r + U\acute{r}) \cdot \sin\alpha - (P_z + E_z - F_z + V\acute{r}) \cos\alpha \quad (11)$$

with initial conditions $t = 0$: $w = w_0$, $\alpha = \alpha_0$,

where $k_c = 0.5C\pi r_p^2 \rho_1$; U, V – projections of the velocity vector of the carrier medium $\mathbf{V}_1$, on the axes r and z; $r' = \frac{3}{r_p}\frac{dr_p}{dt}$

Parameters included in the right parts of equations (10) and (11) P_i, and E_i (at i = r,z) are determined by the projections of the speed of the carrier medium U, V and their space derivatives $\partial/\partial r$, $\partial/\partial z$ on the trajectory of the particle and are calculated by the relations given in [10]**.** The current value of the particle radius r_p and parameter $\acute{r}$ is determined from the solution of the problem of heat

conduction for a spherical particle during evaporation from its outer surface. The parameters F_i in (11) are determined in the general case by the formulas

$$F_r = \frac{gD}{V_{10}^2}\left(1-\frac{\rho_1}{\rho_2}\right)\sin\varphi\,,\ F_z = -\frac{gD}{V_{10}^2}\left(1-\frac{\rho_1}{\rho_2}\right)\cos\varphi,$$

where φ – angle between the z-axis and the direction of the gravity vector (at work φ=0).

Mathematical model of a non-stationary problem of heat conduction in a dispersed spherical particle moving in a carrier medium with a temperature inhomogeneous over the reactor volume T_1, includes[11]:

- heat equation $(\tau > 0,\ 0 < r < r_p)$

$$(c_{p2}(T)\rho_2(T))\frac{\partial T_2}{\partial t} = \frac{1}{r^2}\frac{\partial}{\partial r}\left(\lambda_2(T)r^2\frac{\partial T_2}{\partial r}\right), \quad (12)$$

- initial condition at t = 0:

$$T_2 = T_{20}; \quad (13)$$

- border conditions:

at $r \to 0$:

$$\frac{\partial T_2}{\partial r} = 0\,; \quad (14)$$

at $r = r_p$:

$$-\lambda_2(T)\frac{\partial T_2}{\partial r} = Nu_p\frac{\lambda_1}{2r_p}(T_1 - T_2) - \varepsilon\sigma T_2^4 + q_r\,, \quad (15)$$

here r_p – time-varying particle radius, m; Nu_p - dimensionless heat transfer coefficient on the particle surface; λ_1, λ_2 – thermal conductivity coefficients of the carrier medium and particle material, W/(m K); ε – emissivity; σ – Stefan-Boltzmann constant; q_r – external radiant heat flux, W/m^2.

To take into account phase transformations, additions and changes were made to the mathematical model of the heat conduction problem for a particle [12]:

- when the melting temperature is reached T_L in the particle, a front of phase transformations appears, to determine the speed of movement, which can be used the Stefan condition in the form

$$(\lambda_2(T)\frac{\partial T_2}{\partial r})_{r+0} - (\lambda_2(T)\frac{\partial T_2}{\partial r})_{r-0} = \rho_2(T)L_m\frac{\partial r}{\partial t}\,, \quad (16)$$

L_m – heat of fusion (solidification) of particle material, J/kg;

- upon reaching the evaporation temperature on the surface T_{2V} and the need for calculation with a changing particle diameter, the boundary condition (15) taking into account the Stefan condition takes the form at $r = r_p$:

$$-\lambda_2(T)\frac{\partial T_2}{\partial r} = Nu_p\frac{\lambda_1}{2r_p}(T_1 - T_2) - \varepsilon\sigma T_2^4 + q_r - \rho_2(T)L_v\frac{\partial r_p}{\partial t}\,, \quad (17)$$

where r – radius, m; c_{p2} – heat capacity of particle material, J/(kg K); L_v – heat of evaporation, J/kg.

At $T(r_p) < T_{2V}$ in the condition (17) L_v = 0.

In order to use in the future a finite-difference scheme of through counting without separating the phase transition front [11], in this work, to solve the problem of heat conduction in a particle with melting, a method is used based on the introduction of the effective heat capacity of the particle c_{eff}, depending on temperature and taking into account the thermal effect of phase transformation when the particle reaches the corresponding melting temperature range

$$c_p2 = c_{eff}(T) = \begin{cases} c_l(T), \text{ at } T > T_l; \\ c_s(T_s) + L_m/(T_l - T_s), \text{ at } T_s \le T \le T_l; \\ c_s(T), \text{ at } T < T_s, \end{cases} \quad (18)$$

where T_s and T_l – temperature values that determine the melting zone of the particle material separating the solid and liquid phases; $c_s(T)$ and $c_l(T)$ – heat capacities of the material of the particle, respectively, in the solid-phase and liquid-phase state.

3. Results and discussion

The solution of the three interrelated problems formulated above is performed numerically by the finite-difference method. The problem of hydrodynamics and heat transfer for the carrier medium (1)-(8) was solved in variables vortex – stream function – temperature by the method of alternating directions. The system of nonlinear equations for a particle (10)-(11), written in a difference form, was solved by Newton's method. To solve the problem of heat conduction in a dispersed particle (12)-(18), an implicit difference scheme and the sweep method were used.

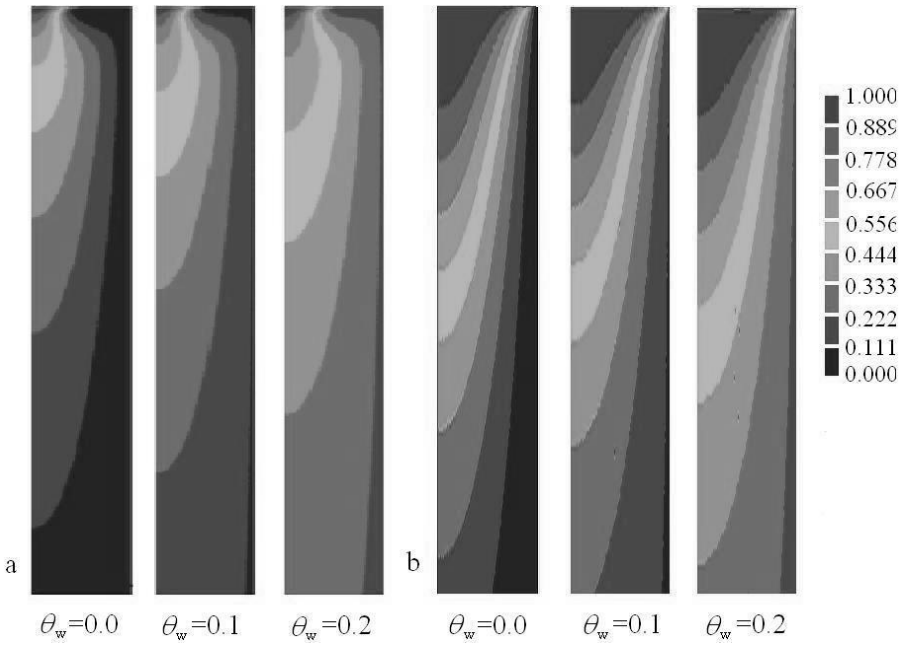

Figure 3 Temperature distribution patterns in plasma for two variants of plasma entry into the reactor at different values of the side wall temperature

There are some results of numerical simulation for spherical silicon particles. The thermophysical properties of silicon used in the calculations were assumed to depend on temperature.

Figure 3 shows the calculated temperature fields in the air plasma at Pr = 0.7 for two schemes of gas supply to the reactor at three different side surface temperatures θ_w. It can be seen that an increase in the temperature of the side surface significantly increases the length of the high-temperature inlet section. It should also be noted that the supply of plasma to the reactor according to the scheme of Figure 3b is more preferable compared to the scheme (Figure 3a), since it allows for a more uniform temperature distribution over the reactor cross section and a greater length of the high-temperature core of the gas flow. The calculation results presented below were obtained with the plasma entering the reactor according to the scheme of Figure 3b.

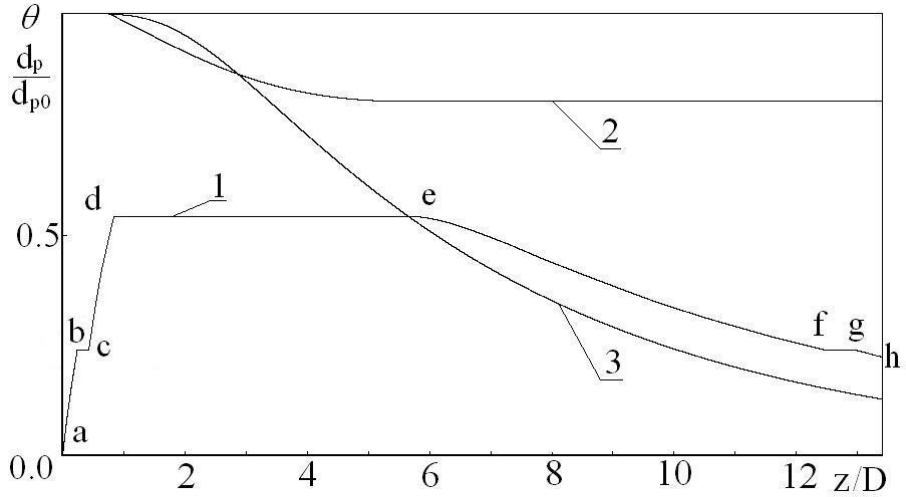

Figure 4 Graphs of changes along the length of the reactor particle surface temperature (1), particle diameter (2) and gas temperature (3) on the trajectory of the silicon particle with d_{p0}=100 μm at T_{10} = 6273 K and V_{10} = 2.9 m/s

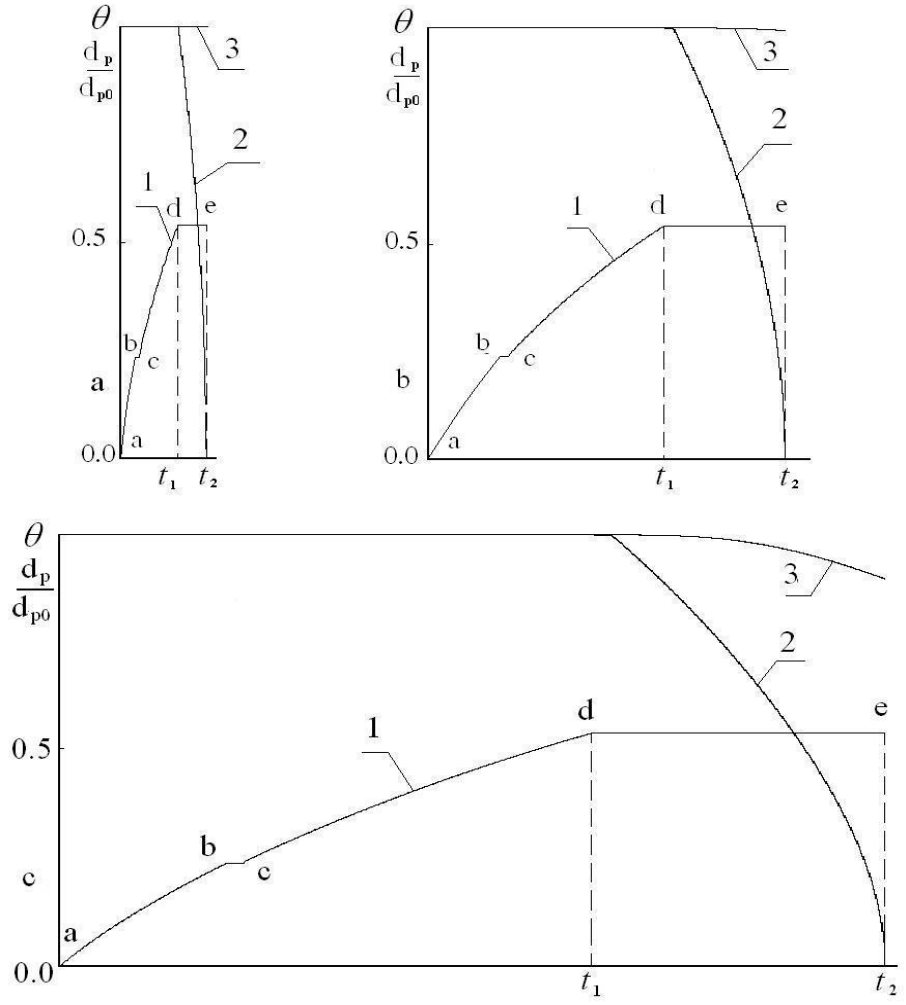

Figure 5 Changes in time of surface temperature (1) and particle diameter (2) and gas temperature (3) on the trajectory of silicon particles with an initial diameter of 20 μm (a), 40 μm (b) and 60 μm (c) at T_{10} = 6273 K and V_{10} = 2.9 m/s

Figure 4 along the length of the reactor shows the calculated dependences of the relative values of the surface temperature of the dispersed particle (1), the particle diameter (2) and the temperature of the carrier air (3) for a particle with an initial diameter dp_0=100 μm at the temperature and air velocity at the reactor inlet, respectively, T_{10} = 6273 K and V_{10} = 2.9 m/s. It can be seen that on the graph of particle temperature change (1) there are sections corresponding to different stages of particle processing: a-b – heating to the melting temperature; b-c – melting; c-d is heating up to the evaporation temperature; d-e – evaporation of a substance from the surface of a particle and a decrease in its diameter and mass; c-f – cooling to the melting point; f-g – solidification of the particle; g-h – further cooling.

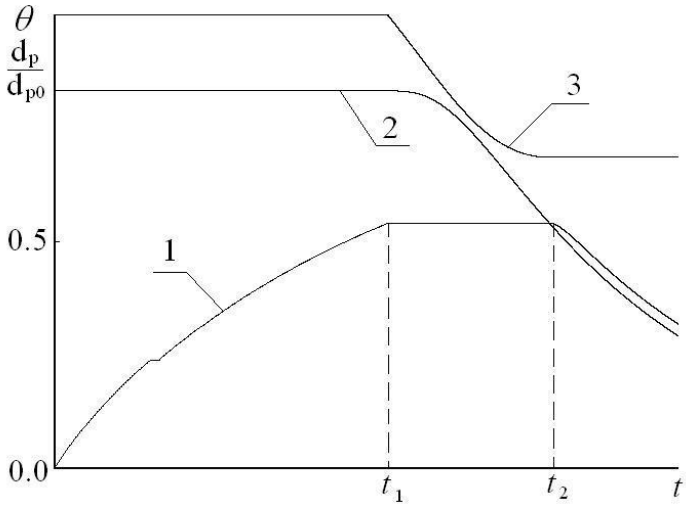

Figure 6 Time variation of surface temperature (1) and particle diameter (2) and gas temperature (3) on the trajectory of silicon particles with d_{p0}=60 μm at T_{10} = 5273 K and V_{10} = 1.135 m/s

Figure 5 shows graphs of time variations of the same parameters as in Figure 4 for completely evaporating silicon particles with initial diameters d_{p0}=20 μm (Figure 5a), 40 μm (Figure 5b) and 60 μm (Figure 5c) and under the same operating conditions. Points of time marked on the graphs t_1 and t_2, correspond to the heating time to the evaporation temperature and the time of the entire process until the particle is completely evaporated. When plotting graphs in Figure 5 and Figure 6 during the evaporation period from t_1 to t_2 time scale decreased by 20 times. In Figure 5a – t_1=0.14 ms, t_2=1.54 ms; Figure 5b – 0.62 ms, 6.16 ms; Figure 5c – 1.38 ms, 15.5 ms.

4. Conclusions

The results of numerical simulation show that in the considered range of regime parameters, the main influence on the time of complete evaporation of the initial dispersed silicon particles is exerted by the value of the gas temperature at the reactor inlet. High temperatures provide large temperature drops across the surface of the particles and, consequently, high heat fluxes, which rapidly heat the particles. An increase in the mass flow rate of the plasma-forming gas practically does not lead to a change in the time of complete evaporation of particles. This is due to the fact that with an increase in the gas flow rate, the length of the high-temperature inlet section in the reactor channel increases, but the velocity of the plasma also increases proportionally. Since the relative velocity of the particle and the plasma flow is small, the residence time of the particle in the high-temperature zone does not increase. Calculations showed that the length of the high-temperature inlet section of the reactor strongly depends on the heat transfer on the lateral surface. Since the heat losses to the wall mainly depend on the temperature difference between the core of the gas flow and the wall, it is advisable to achieve an increase in

operating temperatures on the reactor wall. This is possible if the reactor walls are made of materials with high thermal stability.

As a result of numerical calculations, it was found that in order to evaporate large-diameter dispersed particles, it is necessary to increase the contact time of the particles with the high-temperature core of the plasma jet. This is possible by organizing the supply of the initial material towards the plasma flow, which can also lead to the intensification of convective heat transfer on the particle surface.

The proposed mathematical model and software package make it possible to determine by calculation the geometric and operating characteristics of plasma generators designed for high-temperature processing of dispersed materials in order to obtain ultrafine powders with desired properties and nanoscale.

Acknowledgements

The work was supported by the Russian Foundation for Basic Research (project 08-08-00831-a).

References

[1] 1. Kurkin E.N., Shulga Yu.M., Domashnev I.A. Plasma-chemical synthesis and properties of nanosized particles from the Cr2 O3 – Al2O3 system // Alternative Energy and Ecology, 2007, No. 8(52). – p. 25-30.

[2] 2. Timoshenkov S.P., Prokopiev E.P. Dyachkov S.A. Synthesis of fine powders in high-frequency plasma // Physics and chemistry of material processing, 2002, No. 5. – p. 26-32.

[3] 3. Mosse A.L., Burov I.S. Processing of dispersed materials in plasma reactors. – Minsk: Science and technology, 1980. – 208 p.

[4] 4. Rykalin N.N., Sorokin L.M. Metallurgical high-frequency plasma torches. Electro- and gas dynamics. – M.: Nauka, 1987. – 168 p.

[5] 5. Agafonov K.N., Alekseev N.V., Samokhin A.V., Kurkin E.N. Experimental and numerical study of the process of formation of ultrafine powder of titanium oxide in a channel plasma-chemical reactor // Teor. main chem. tech., 1996, Vol. 30, No. 1. – p. 79-84.

[6] 6. Pustovoitenko A.I., Panfilov S.A., Tsvetkov Yu.V. Mathematical model of the jet-plasma process of processing dispersed raw materials with the production of condensation powder // Physics and Chemistry of Materials Processing, 1979, No. 2. – p. 62-69.

[7] 7. Polezhaev V. I., Bune A. V., Verezub N. I. et al. Mathematical modeling of convective heat and mass transfer based on the Navier-Stokes equations. – M.: Nauka, 1987. – 272 p.

[8] 8. Novoselov V.S. Analytical mechanics of systems with variable masses. – L: Publishing house LOLGU, 1969. – 240 p.

[9] 9. Kholpanov L. P., Ismailov B. R., Vlasak P. Modeling of Multiphase Flow Containing Bubles, Drops and solid Particles // Eng. Mech., 2005, Vol. 12, no. 6. – p. 1-11.

[10] 10. Nekrasov A.K., Kholpanov L.P., Nekrasova E.I. Mathematical modeling of the dynamics of the dispersed phase under nonisothermal free convection of a heterogeneous medium in a vertical cylindrical reactor // Teor. main chem. tech., 2008. V. 42, No. 2. – p. 152-159.

[11] 11. Samarsky A.A., Vabishchevich P.N. Computational heat transfer. – M.: Editorial URSS, 2003. – 784 p.

[12] 12. Nikitenko N.I. Conjugate and inverse problems of heat and mass transfer. – Kyiv: Nauk. Dumka, 1988. – 240 p.